Hydration of Ferrite-Rich Portland Cement: Evaluation of Fe-Hydrates and Fe Uptake in Calcium-Silicate-Hydrates

Natsumi Noguchi [1], Krishnya Siventhirarajah [1], Takashi Chabayashi [2], Hiroyoshi Kato [2], Toyoharu Nawa [1], Yogarajah Elakneswaran [1, *]

[1] Division of Sustainable Resources Engineering
Faculty of Engineering, Hokkaido University
Kita 13, Nishi 8, Kita-ku, Sapporo, 060-8628, Japan

[2] Development Department, Cement Business Division,
Tokuyama Corporation, Yamaguchi, Japan

* Corresponding author
E-mail: elakneswaran@eng.hokudai.ac.jp
Tel: +81-11-706-7274

Abstract

The hydration process in ferrite-rich cement (FC) and its pore structure have been investigated by experimental and thermodynamic modelling techniques. X-ray diffraction (XRD)/Rietveld analysis, thermogravimetry (TG), and mercury intrusion porosimetry (MIP) were performed to study the hydration process, pore volume-pore size distributions, and Fe uptake in calcium-silicate-hydrate (C-S-H). Similar phases were found in both FC and ordinary Portland cement (OPC). The hydration degree of FC was higher at the early stage compared with that of OPC; however, the hydration of OPC exceeded that of FC after 14 days because the high amount of C_2S in OPC promoted the late hydration. The XRD-TG results revealed relatively similar Fe uptake by C-S-H in both FC and OPC. The thermodynamic model confirmed the formation of a high amount of Fe phases in FC. Moreover, the model predictions agreed well with the experimental results, demonstrating the accuracy of the proposed model for FC.

Keywords: Ferrite-rich cement (FC); hydration; Fe phases; calcium-silicate-hydrate (C-S-H); thermodynamic modelling

1. Introduction

Concrete is the second most used material in the world after water [1]. Due to the significant increase in the demand and production of cementitious materials, (the worldwide production has approximately doubled between 2005–2015 [2]), the global CO_2 emissions increase daily, thereby posing several environmental risks. Cement manufacturing plants are responsible for approximately 8–9% of anthropogenic CO_2 emissions and approximately 1 tonne of CO_2 are produced during the production of 1 tonne of cement [3-5]. In addition, high amount of thermal energy is required for the production process (approximately 4.7 million British Thermal Unit per 1 tonne of cement) [2]. Recently, there have been considerable developments to reduce CO_2 emission and to increase energy savings in the cement and concrete industry. It includes the developments of supplementary

cementitious materials, production of alternative clinkers with reduced amounts of limestone in the raw mix, alternative fuels and renewable energy sources, and process optimisation [3, 5-7].

Very recently, the reduction of the firing temperature of the clinker has been proposed and investigated to reduce energy consumption and CO_2 emission [8-9]. In this process, the clinker has been produced alternatively, by reducing the firing temperature of the clinker by 100 °C, which varies from the production of conventional ordinary Portland cement (OPC) wherein the burning temperature of the clinker is 1450 °C. The clinker burnt at 1350 °C consists of higher amount of ferrite (C_4AF) (approximately twice) and lower amounts of belite (C_2S) (approximately half) compared to those in OPC. This novel cement produced on the aforementioned low-temperature basis is called ferrite-rich Portland cement (FC). It should be noted that the same raw materials as used for OPC have been used to produce FC, but the ratio of the raw materials has been adjusted to achieve the target mineral composition of FC. Further, it has been demonstrated that the FC can reduce approximately 5 % of CO_2 emission compared to OPC during the clinkering process [8]. Although the FC has been proven to be an eco-friendly alternative to OPC, the number of studies on the subject are very limited [10-12], providing insufficient information on the hydration process, evolution of mechanical properties and performance of FC, which restricts the commercialisation, industrial applications and particularly the developments of numerical models.

The application of thermodynamic models coupled with an accurate database have gained significant momentum to accurately investigate the hydration process of a large variety of cement pastes with wide range of variables such as temperature, water to cement ratio and relative humidity [13-16]. Basically, chemical behaviours of numerous minerals and phases existing in the hydrated cement are thermodynamically well defined. However, the necessary thermodynamic data for Fe phases are still very limited. Besides, the experimental characterisation of Fe phases is complicated, as the signals from Fe phases in hydrated cement significantly overlap with those of the Al analogues using typical

techniques such as X-ray diffraction (XRD), thermogravimetric analysis (TGA) and scanning electron microscopy [13, 17]. The identification of amorphous Fe phases in the hydrated cement matrix is also difficult using conventional techniques. In addition, Fe(III) could partly substitute Al(III)-bearing hydrates such as Fe-ettringite, Fe-monosulfate, Fe-monocarbonate, Fe-hemicarbonate and Fe-siliceous hydrogarnet depending on the presence of calcium, sulphate or carbonate during cement hydration [13, 18-19]. As experimentally demonstrated by Dilnesa et al [13], Fe/Al-siliceous hydrogarnet ($C_3(A,F)S_{0.84}H_{4.32}$) is more stable than Fe-containing AFm phases and Fe-ettringite in OPC. Moreover, the leaching of Ca from C-S-H and the low Ca/Si ratio induce the uptake of Fe^{3+} ions in the place vacated by calcium [20-21]. However, a recent study showed that the uptake of Fe^{3+} ions occurs highly at high Ca/Si ratios (1.2 and 1.5) of synthesised C-S-H [19]. At high Ca/Si ratios, the presence of Fe^{3+} ions is witnessed in the interlayer of C-S-H phases. On the other hand, the uptake of Fe^{3+} ions by the interlayer is eliminated at a low Ca/Si ratio (0.8), instead, leading to the formation of Ca-Si-rich complex on the surface of C-S-H. With all the above contrast observations, the mechanism of Fe(III) uptake by C-S-H is poorly understood and remains ambiguous.

In our previous work [10], we have studied the hydration behaviour of FC and compared it with that of OPC. However, we did not identify or quantify the Fe-hydrates in the cements. Therefore, the objectives of this study were (i) to investigate the hydration process of FC and quantify Fe-hydrates and (ii) to evaluate Fe uptake by C-S-H. All the experimental results were synergistically used to verify the coupled thermodynamic model developed in our previous work [22] to predict the hydration products including the Fe-siliceous hydrogarnet and Fe uptake by C-S-H (C-F-S-H).

2. Materials and methods

2.1 Experimental procedure

OPC and ferrite-rich Portland cements were used in this study. The physical properties and the mineral composition of the cements are tabulated in **Table 1**, and the chemical composition of oxide

and the proportions of raw materials are given in Table 1 of ref. [10]. The cement was mixed with distilled water at a water to cement ratio of 0.5. The mixture was stirred manually until the bleeding stopped. Further, it was cast into cylindrical moulds and sealed-cured at 20 ºC. The samples that reached the predetermined curing time (1, 6, and 12 h and 1, 2, 3, 7, 14, 28, 91 and 182 days) were ground and immersed in acetone for 1 h to stop the hydration. Thereafter, the samples were removed from the acetone solution by suction filtration using an aspirator. Finally, the samples were kept in an oven at 40 ºC until they reached a constant mass. The prepared samples were ground and powdered for XRD and TG measurements. The selective dissolution experiment was performed according to the method proposed by Dilnesa et al. [13]. In the selective dissolution method, 5 g of a crushed hydrated cement sample was stirred for 2 h using a magnetic stirrer in a beaker containing 300 mL methanol and 20 g salicylic acid. The suspension was allowed to settle for approximately 15 min and then it was vacuum-filtered through 0.08-mm filter paper. Thereafter, the samples were dried at 90 °C for 45 min in an electric furnace. The XRD/Rietveld analysis was performed to determine the quantities of hydration products and un-hydrated clinker minerals. Rigaku MultiFlex X-ray generator with CuKα radiation was used for XRD measurements while Siroquant Version 4.0, manufactured by Sietronics, was adopted for quantitative Rietveld analysis. The TG-differential thermal analysis (DTA) was conducted using TG/DTA7220 manufactured by HITACHI under an N_2 flow environment. The waiting time before the measurement for stabilising the apparatus was 50 min. The temperature was raised at a rate of 5 °C/min from 20 to 1000 °C and was maintained for 10 min and then reduced at a rate of 50 °C/min. Approximately 10 mg of the sample was weighed and used for measurements. Mercury intrusion porosimetry (MIP) was conducted using Shimadzu Auto Pore IV 9500 with a pressure range of 0.5–60000 psi. The samples were cut into cubes (3 mm) after curing and immersed in acetone for 24 h. Thereafter, the samples were vacuum-dried for 24 h before conducting MIP measurements.

Table 1: Physical properties and mineral composition of cements used

Cement	**OPC**	**FC**
Blaine specific surface area (cm^2/g)	3220	3220
Density(g/cm^3)	3.19	3.20
LoI	0.80	0.76
C_3S	57.6	59.1
C_2S	18.0	8.6
C_3A	9.0	8.5
C_4AF	9.3	17.2
Gypsum	3.02	2.78

2.2 Modelling approach

The hydrate assemblage of OPC and FC as a function of hydration time was calculated using the thermodynamic model, which couples IPhreeqc module [23] for thermodynamic equilibrium and Microsoft Excel for solving cement hydration. The thermodynamic properties of cement hydrates including Fe-containing phases were collected from Cemdata18 [24-25]. The data were converted to PHREEQC format [22] and used along with PHREEQC default thermodynamic database [26]. The uptake of Fe by C-S-H can be expressed by the distribution coefficient, R_d, which can be defined as follows with reference to the alkali adsorption on C-S-H [27]:

$$\boldsymbol{R_d(mL/g)} = \frac{\boldsymbol{Fe\ in\ solid\ C{-}S{-}H}}{\boldsymbol{Fe\ concentration\ in\ solution}} \quad (1)$$

where *Fe in solid C-S-H* is the amount of Fe uptake by 1 g of C-S-H (mmol/g), and *Fe concentration in solution* is the equilibrium concentration of Fe (mmol/mL).

3. Results and discussion

3.1 Characterisation of cements and Fe-hydrates

Fig. 1 shows the hydration reaction of each clinker mineral and the total hydration degree of cement determined by XRD/Rietveld analysis. The hydration degree of C_3S and C_3A are similar in both cements, and they are fully hydrated after 28 days. However, the hydrations of C_2S and C_4AF in OPC are higher than those in FC. The difference becomes remarkable from 91 days for C_2S and 14 days for C_4AF. The change in the proportions of the clinker minerals affects their hydration degree. These differences did not alter the total hydration degree of cement (**Fig. 1.** (E)). FC shows higher hydration degree up to 7 days, and the high amount of C_2S contributes to the increase in the late hydration of OPC.

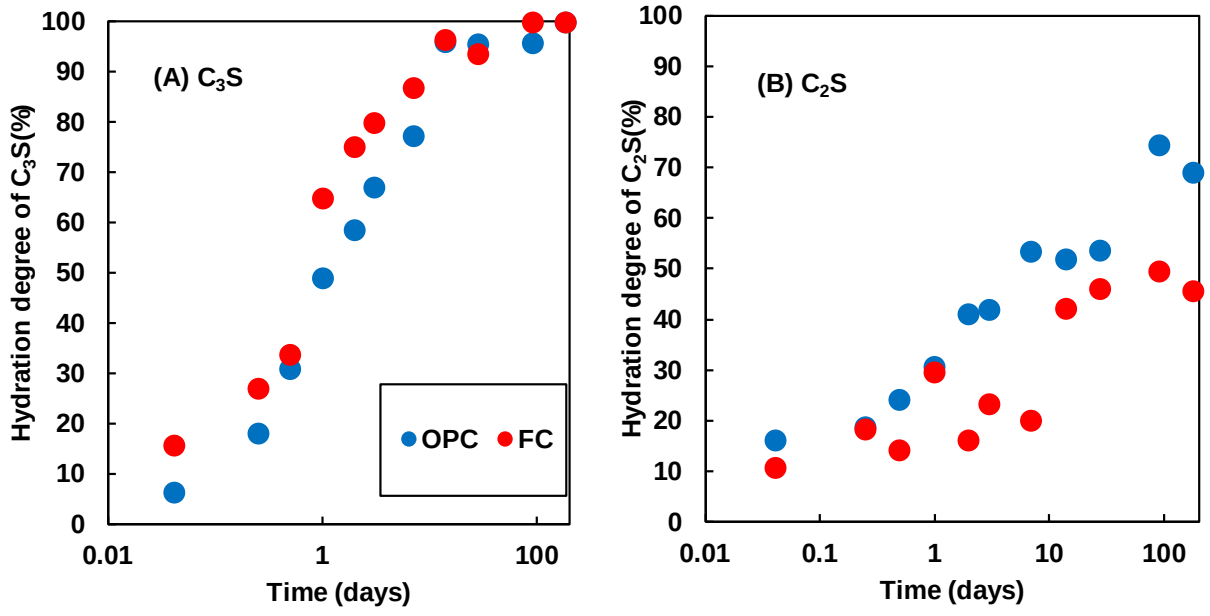

169

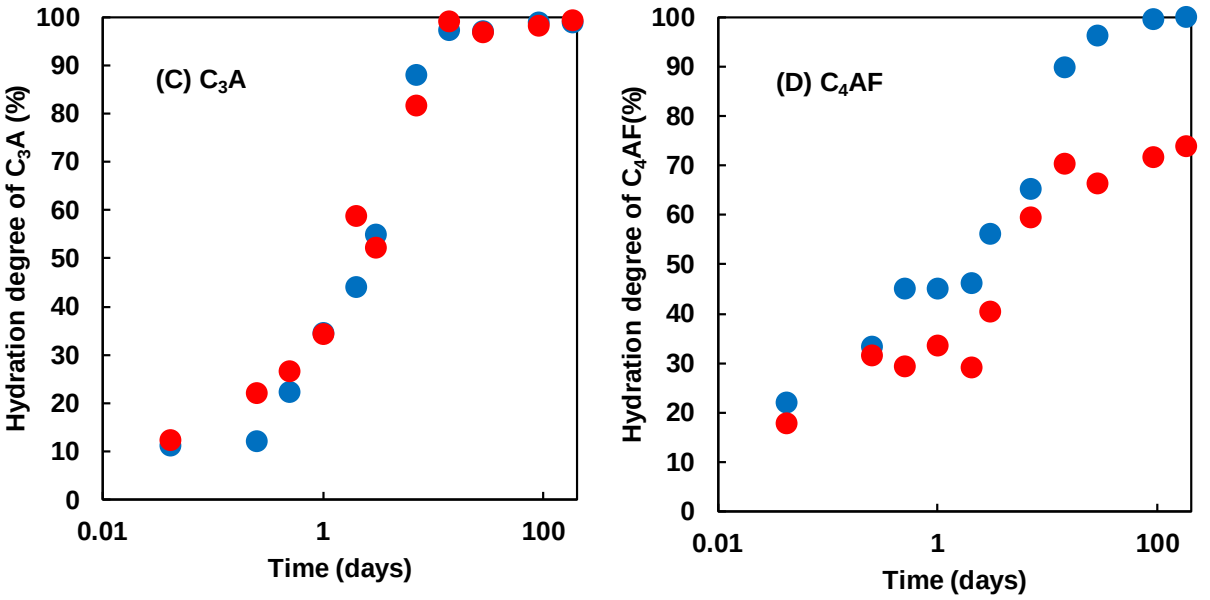

170

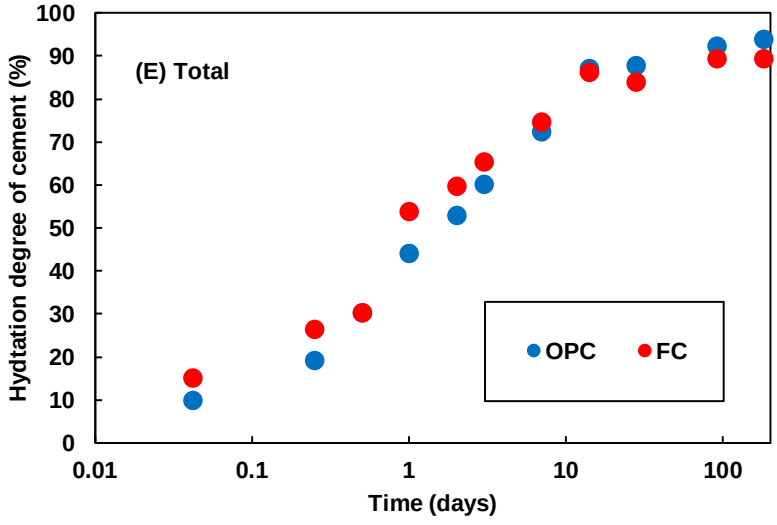

171

172 **Fig. 1.** Hydration of clinkers and cements as a function of time from the XRD/Rietveld analysis

Lothenbach et al. have reported that Fe-siliceous hydrogarnet is the only Fe-containing phase expected to form during the hydration of Portland cements; thus, the presence of other Fe-containing phases in the hydrated cement system can be negligible [24]. To quantify the formed Fe-siliceous hydrogarnet, the selective dissolution was conducted. **Fig. 2** shows the XRD pattern of the sample after the selective dissolution treatment. The peak of siliceous hydrogarnet at approximately 17.5°/2θ and additional peak at 20.2°/2θ and 26.9°/2θ indicated by dotted line can be observed after 7 days of hydration. However, the poor crystallinity of siliceous hydrogarnet makes it difficult to quantify by Rietveld analysis. Therefore, TG/differential thermal gravimetry (DTG) was used to quantify the formed siliceous hydrogarnet. **Fig. 3** shows the TG/DTG curves before and after the selective dissolution treatment of FC hydrated for 28 days. The mass reduction and the remaining phases can be observed after selective dissolution. In particular, the portlandite peak at approximately 400 °C to 450 °C disappears, and the peak of siliceous hydrogarnet is confirmed at approximately 200 °C to 300 °C. These results are consistent with those reported by Dilnesa et al. [13] and proved that the selective dissolution is an effective method to quantify the Fe-containing phases in the hydrated cement. As shown in XRD and DTG results, the peak of C-S-H and AFm phases remain after the selective dissolution, but they do not overlap with the peak of siliceous hydrogarnet to quantify. From the mass loss, the amount of formed siliceous hydrogarnet was calculated, and the results are shown in **Fig. 4** as a function of hydration time. For the calculation, it was assumed that the chemical composition of Fe-siliceous hydrogarnet as $Ca_3FeAl(SiO_4)_{0.84}(OH)_{8.64}$. Approximately 10–12% of Fe-siliceous hydrogarnet was formed in the hydrated cements, primarily at the early stages of hydration. The hydration degree of ferrite correlates to the formation of Fe-siliceous hydrogarnet, and the high content of ferrite in FC leads to the formation of a high amount of Fe-siliceous hydrogarnet at the same hydration time. As reported in ref. [13, 16-17], the cement hydration produces iron hydroxides during the first hours and then siliceous hydrogarnet after 1 day and longer. The results (**Fig. 4**)

showed that the amount of formed Fe-siliceous hydrogarnet is almost constant after 14 days of hydration.

The measured porosity and pore size distribution for hydrated cement are shown in **Fig. 5**. OPC and FC hydrated for 7 and 182 days are shown in **Fig. 5** as an example. At an early age, FC has a lower amount of pore volume and large amount of smaller pore compared to OPC, but this trend is reversed at the later stages of hydration. Furthermore, the porosity of both cements is similar in the hydration period of 14–28 days. The hydration degrees of clinker minerals, mainly C_2S and C_4AF, affect the microstructure of the hydrated cement paste. The late hydration reaction of high-content C_2S in OPC contributes to the lesser and denser pore structure compared with that of FC. This difference will contribute to the change in mechanical properties of the hydrated cement paste.

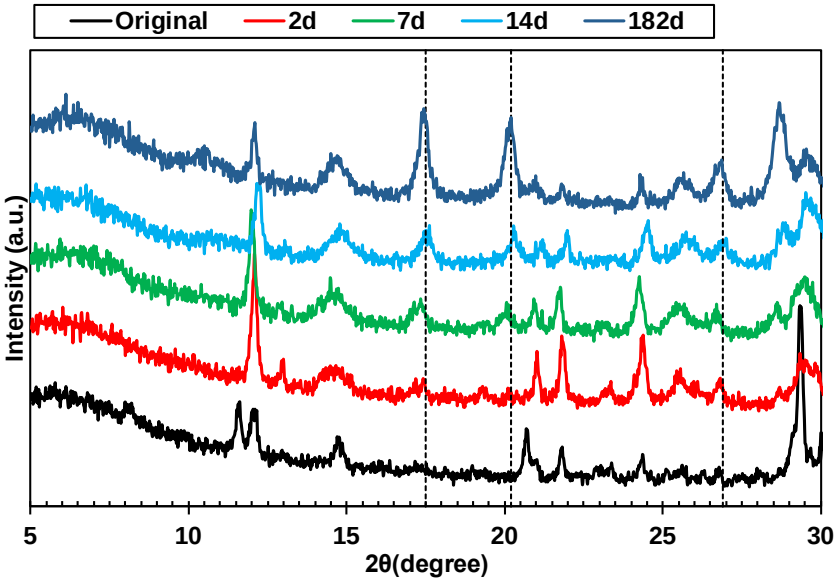

Fig. 2. XRD patterns of OPC after selective dissolution

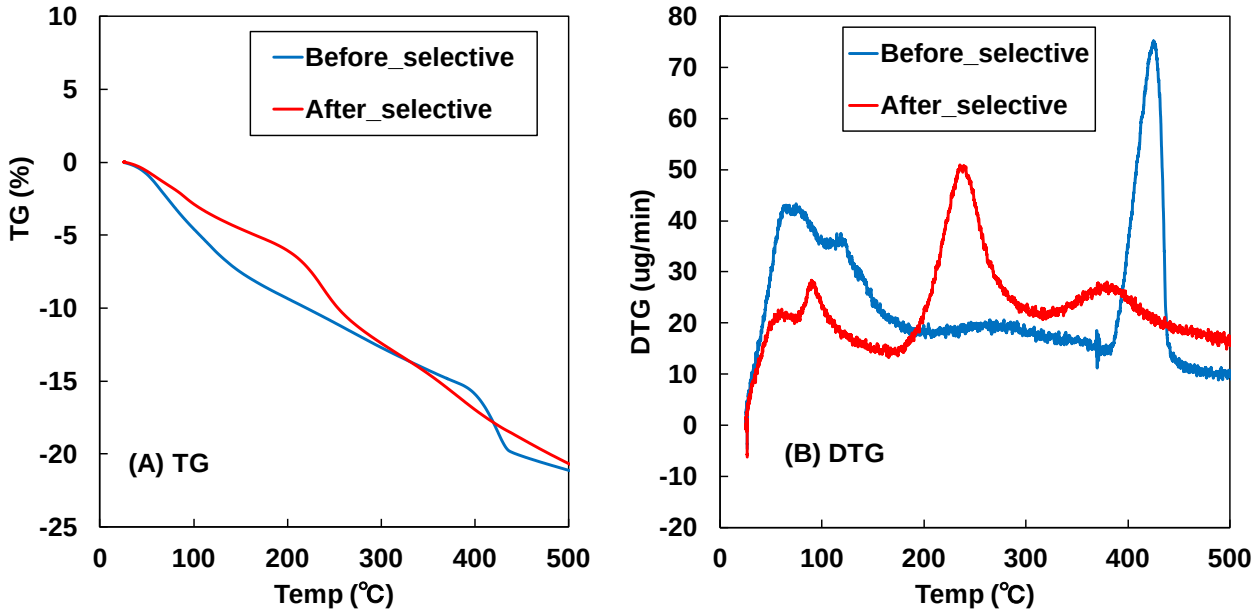

213

214 **Fig. 3.** Effect of selective dissolution after 28 days of hydration of FC. (A) TG; (B) DTG

215

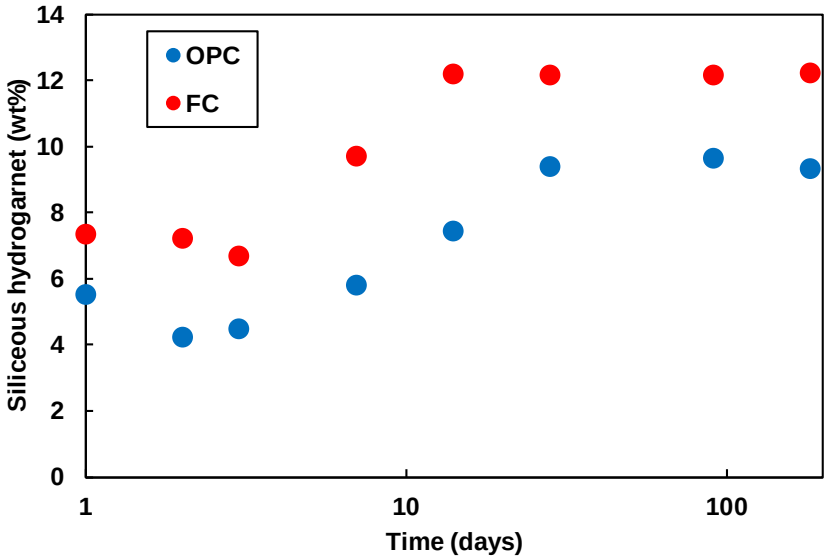

216

217 **Fig. 4.** Amount of siliceous hydrogarnet in the hydrated cements

218

219

220

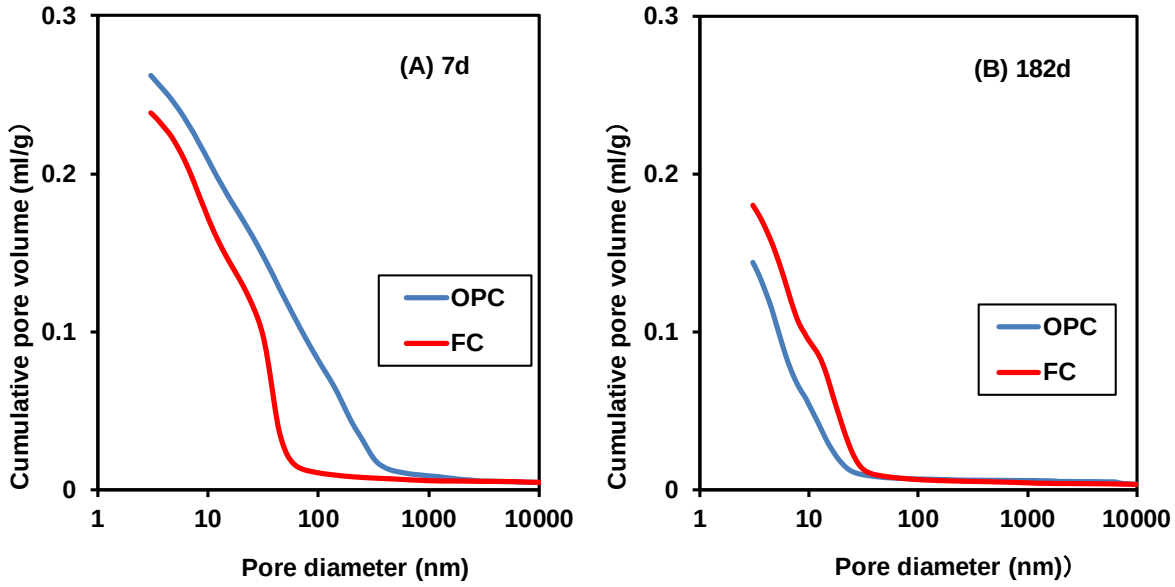

221

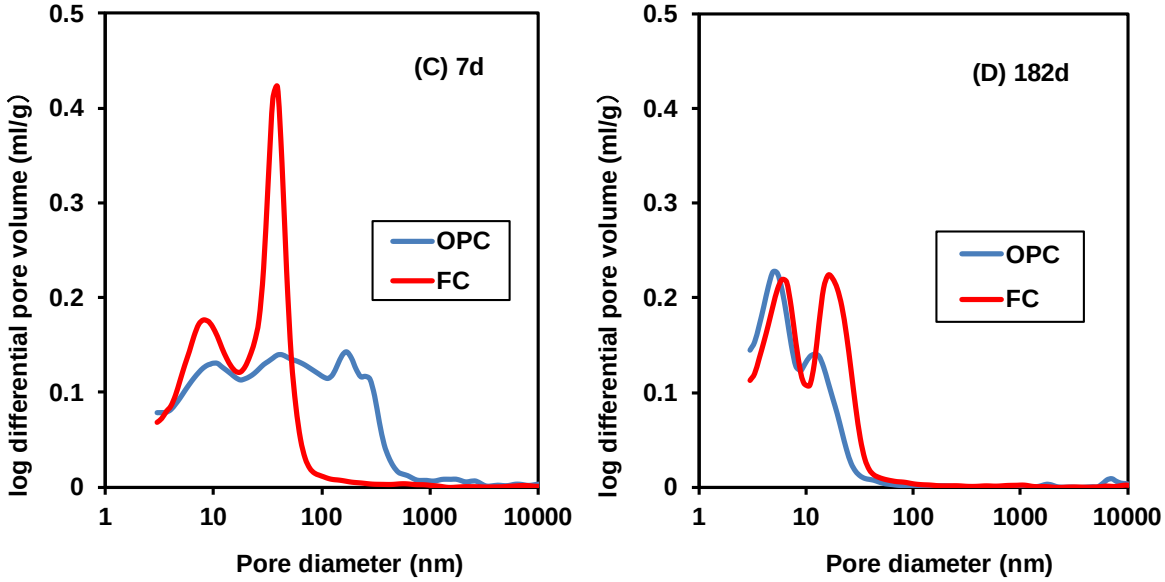

222

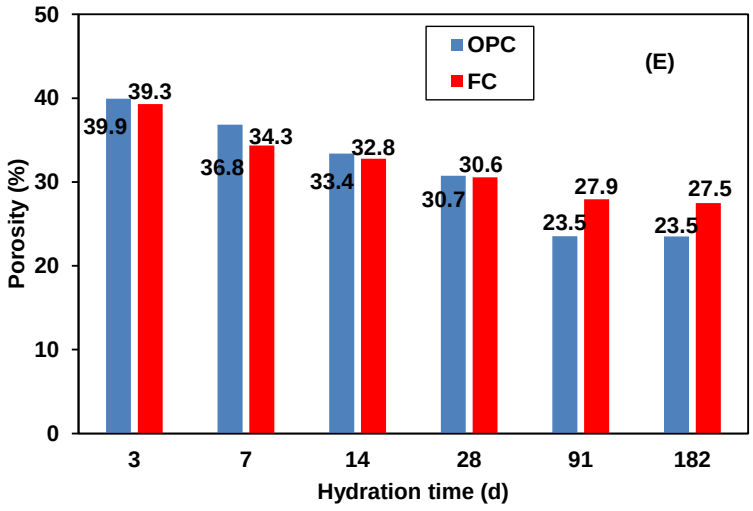

223

224 **Fig. 5.** Cumulative pore volume, pore size distribution and total porosity of OPC and FC

225

3.2 Incorporation of Fe in C-S-H

The recent research on Fe uptake has been focused on the synthetic C-S-H [19], and there is a lack of results or report on Fe incorporation in C-S-H in the hydrated cement. Many studies have shown that the amount of Fe ions in the pore solution is negligible [15, 22]. To find the state of Fe ions in the pore solution after the hydration of C_4AF, a thermodynamic calculation was performed considering various Fe ions and complexes and without considering any Fe-containing hydrate formation. The results show that $Fe(OH)_4^-$ is primarily found in the high-pH pore solution of the hydrated cement (**Fig. 6**), similar to producing $Al(OH)_4^-$ in high-pH solution [19]. Therefore, Fe ions released from the hydration of C_4AF form $Fe(OH)_4^-$ and produce Fe-containing phases or incorporate into C-S-H. Therefore, with the results shown in **Fig. 4**, the amount of Fe taken by C-S-H can be calculated as

$$M_{C-(F-)S-H} = M_{Fe\ dissolved} - M_{Siliceous-Hydrogarnet} \quad (2)$$

where $M_{C-(F-)S-H}$ is the Fe uptake by C-S-H (mol), $M_{Fe\ dissolved}$ is the amount of Fe released from the hydration of C_4AF (mol), and $M_{Siliceous-Hydrogarnet}$ is the Fe in Fe-Siliceous hydrogarnet (mol).

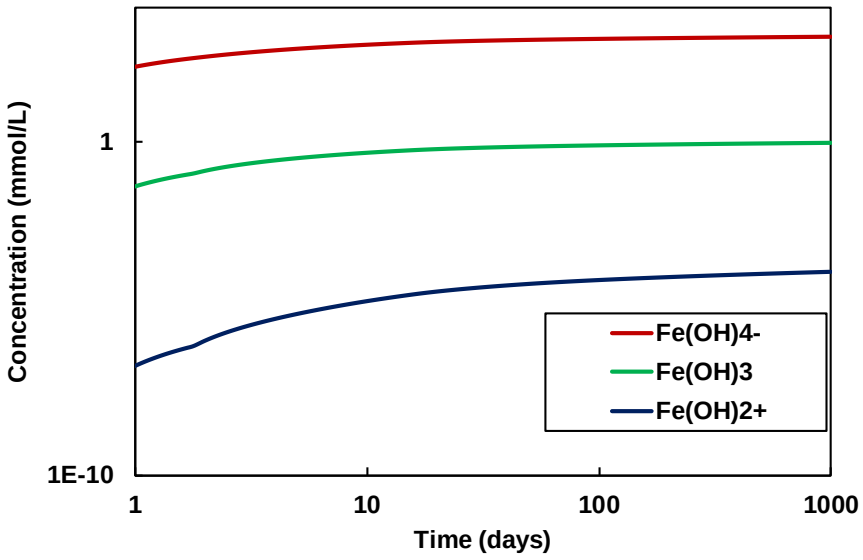

Fig. 6. Calculated concentrations of Fe complexes as a function of hydration time in OPC

The calculated mol percentages of Fe in C-S-H and Fe-siliceous hydrogarnet as a function of hydration time for both cements are shown in **Fig. 7.** Initially, the released Fe from C_4AF forms as Fe-siliceous hydrogarnet, and then the released Fe incorporates into C-S-H. Both cements show a nearly equal amount of Fe uptake by C-S-H. The Fe incorporation into C-S-H was considered by the distribution ratio, R_d, together with thermodynamic calculations. The calculated R_d values as a function of Fe concentration is shown in **Fig. 8**. The distribution coefficient decreases with increase of Fe concentration and follows power approximation, as proposed for alkalis [28]. In the construction of the model, it is desirable to have a single equation for adsorption irrespective of cement type. Therefore, in **Fig. 8**, R_d values of both cements have been used to drive the equation. The results indicate the decrease of Fe uptake by C-S-H with the increase in Fe concentration. Mancini et al. have reported a relationship between sorbed Fe and aqueous solution Fe from the sorption experiment on synthesised C-S-H with Ca/Si ratio of 0.8 and 1.5, and their results showed that R_d depends neither on the composition of C-S-H nor the pH of the solution [19]. In this study, R_d does not depend on cement type, but it relates to the equilibrated Fe concentration in the pore solution.

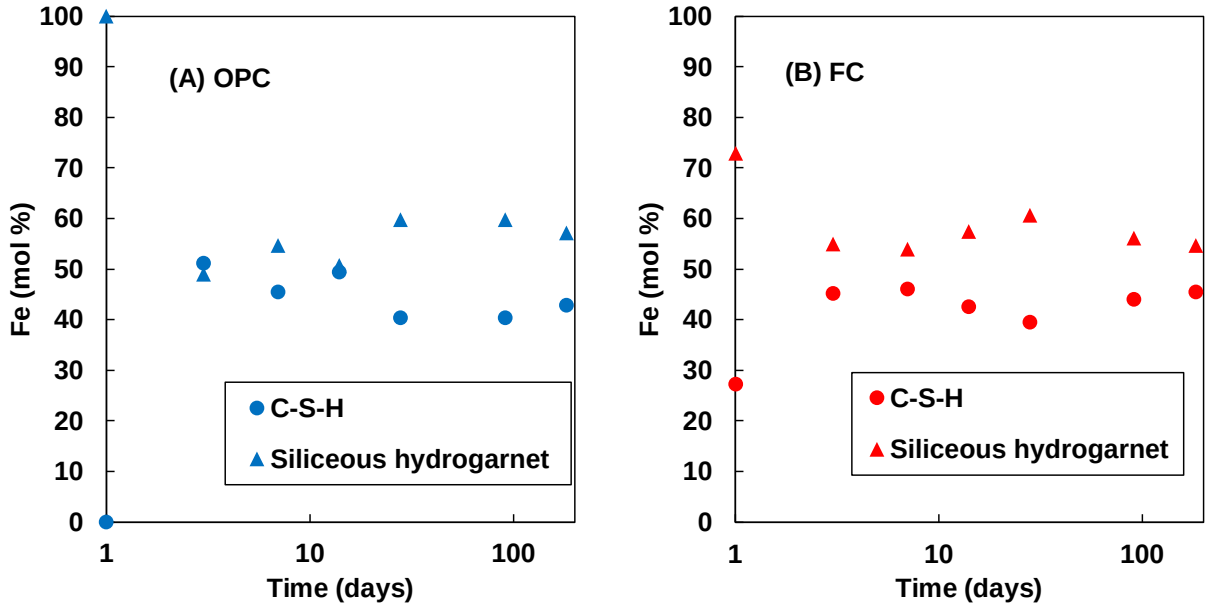

Fig. 7. State of Fe in (A) OPC; (B) FC

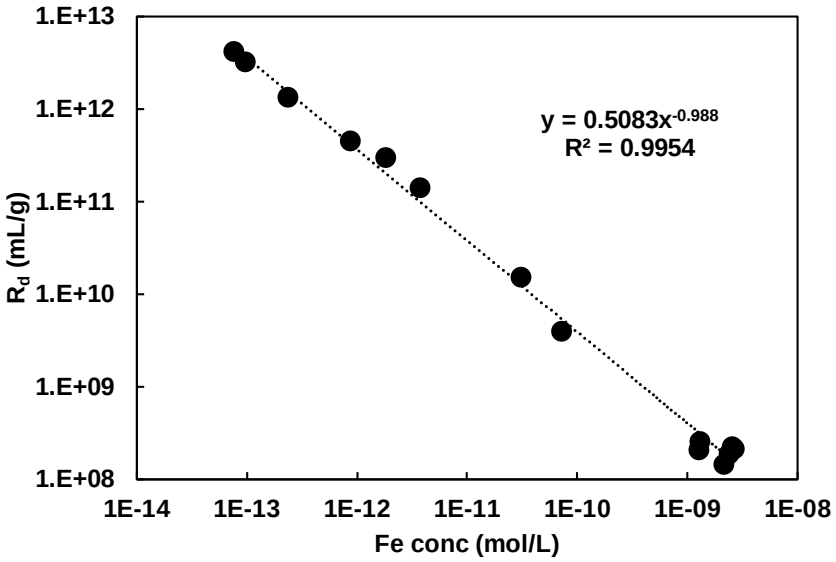

262

263 **Fig. 8.** Relationship between distribution coefficient and concentration of Fe

264

265 Various mechanisms have been proposed for aluminium incorporation into C-S-H, including the
266 substitution of Si atom at bridging sites (Q^2B) of the aluminosilicate chains or cross-linked sites (Q^3),
267 exchange with interlayer calcium ions, and surface complexation reactions [29-30]. A similar
268 mechanisms can be considered for the uptake of Fe by C-S-H. Mancini et al. have analysed the uptake
269 mechanism based on ^{29}Si NMR and EXAFS data and showed that the coordination of Fe into C-S-H
270 depends on its Ca/Si [19]. As shown in **Fig. 6.**, Fe (III) exists mainly as $Fe(OH)_4^-$, and the possible
271 exchange with interlayer calcium would not easily occur. Furthermore, the Fe sorption by C-S-H
272 depends on the equilibrium concentration, and therefore, the surface complexation is the main
273 mechanism for the uptake of Fe by C-S-H. Hass et al. have proposed surface complexation
274 mechanism for aluminium uptake through $Al(OH)_4^-$ [31], and $Fe(OH)_4^-$ can adsorb on C-S-H in a
275 similar way as aluminium. The hydrated cement pore solution has a high-pH and high Ca
276 concentration, which is responsible for the positive surface charge on C-S-H through a high
277 concentration of calcium adsorbed surface specie, $\equiv SiOCa^+$ [31-32]. It is believed that $Fe(OH)_4^-$ can
278 adsorb on $\equiv SiOCa^+$ as follows:

279

280 $$\equiv SiOH + Ca^{2+} + Fe(OH)_4^- \leftrightarrow \equiv SiOCa\ Fe(OH)_4 + H^+ \quad (3)$$

3.3 Thermodynamic model and verification

The coupled thermodynamic model developed in our previous study was used to predict the hydrate assemblage as a function of hydration time [10, 22]. The relationship derived in **Fig. 8.** was incorporated into the model to account for Fe uptake by C-S-H in the hydration of cement. The chemical composition of $(CaO)_{1.667}(SiO_2)$: $2.1H_2O$ with known thermodynamic properties [24-25] was assumed for C-S-H. The model predictions were compared with the experimental results in **Fig. 9** for Fe-siliceous hydrogarnet and other products. It should be noted that experimental results of amorphous and poorly crystalline monosulfate [33] were compared with the addition of the modelling results of C-S-H, Fe incorporated C-S-H, monosulfate, and hydrotalcite which was very small quantity in the hydration product and difficult to quantify accurately by XRD/Rietveld analysis. Despite some variation in OPC, the modelling results of Fe-siliceous hydrogarnet and other hydrates reproduced well the experimental data of both types cement. Both cements produce nearly the equal amount of portlandite and ettringite, but the higher proportion of belite produces more C-S-H in OPC than in FC, and more ferrite in FC produces high Fe-siliceous hydrogarnet. The composition of calculated phase assemblage in terms of weight percentage for both cements are shown in **Fig. 10.** Approximately 2 % of Fe incorporated C-S-H [C-(F)-S-H] was produced in the matured hydrated cement. The amount of formed C-(F)-S-H is very small relative to the ferrite hydration product of Fe-siliceous hydrogarnet and thus, its effect in the physical properties of the paste could be negligible.

The molar volume of each hydration products including Fe-siliceous hydrogarnet helps to estimate the porosity of cement paste. The capillary porosity was calculated by deducting the volume of hydration products and un-hydrated cement, and chemical shrinkage from the initial volume of paste [34]. In the thermodynamic model, the C-S-H was divided into low density (LD) and high density (HD) C-S-H, and the porosity associated with the C-S-H was calculated as gel porosity [34]. As shown in **Fig. 5**, the MIP technique measures the porosity for the pore diameter above 3 nm, which

includes capillary porosity and a part of gel porosity. Therefore, it is appropriate to compare MIP results with the summation of capillary porosity and LD C-S-H gel porosity. The comparison is shown in **Fig. 11** for both cements as a function of hydration period. The modelling results show a relatively good agreement with the measured data.

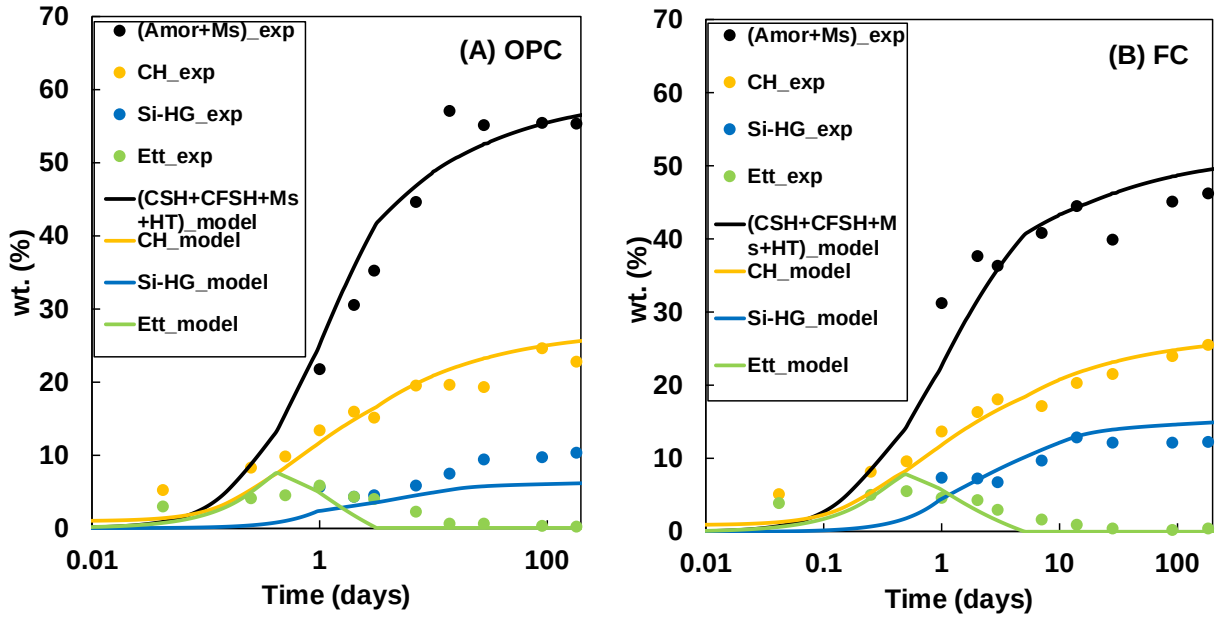

Fig. 9. Comparison of calculated hydrates with the quantitative values determined by XRD Rietveld analysis and TG/DTA for (A) OPC and (B) FC

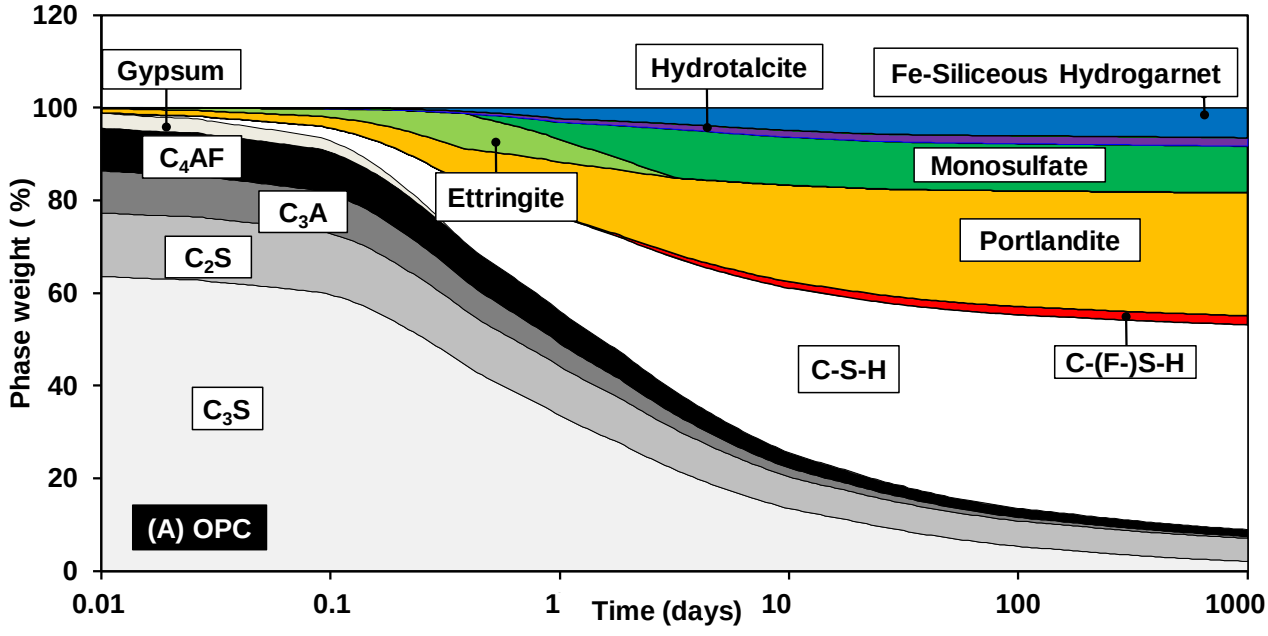

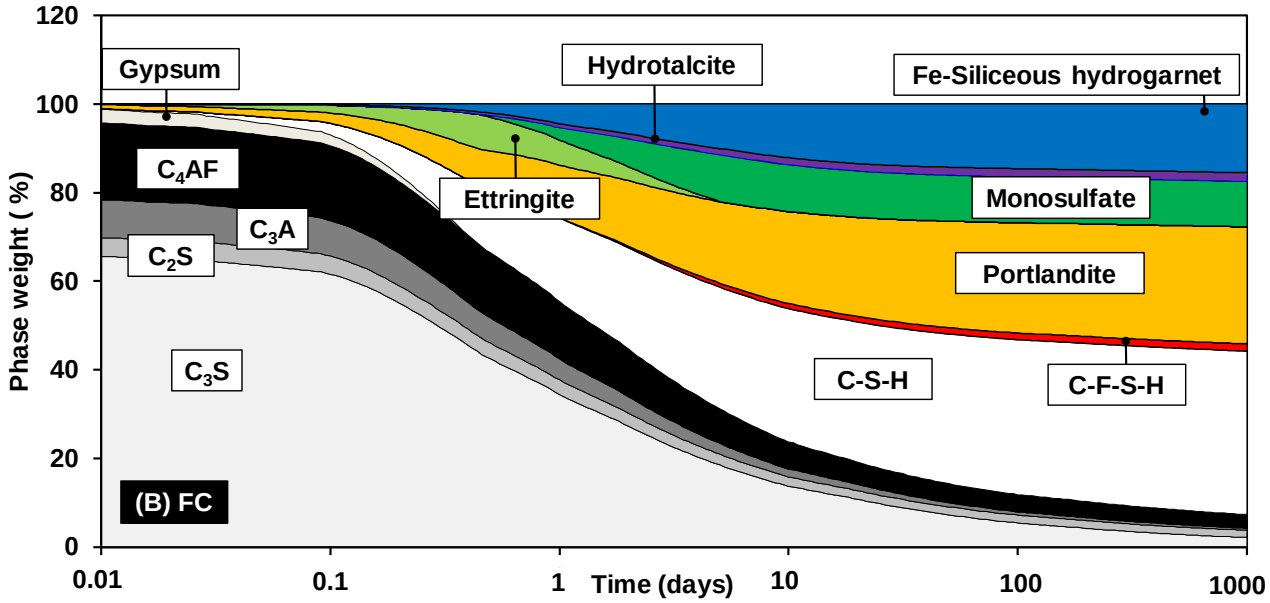

Fig. 10. Calculated mass of hydrates as a function of hydration time for (A) OPC and (B) FC

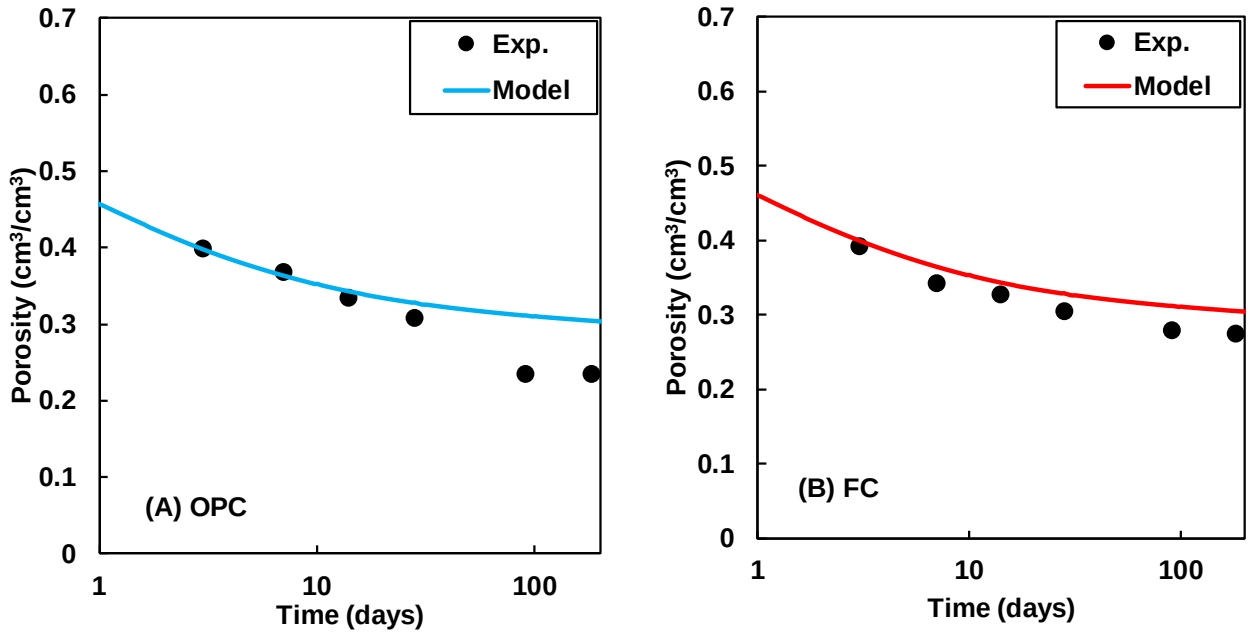

Fig. 11. Comparison of porosity for (A) OPC and (B) FC

4. Conclusions

High proportion of ferrite and low of belite in ferrite-rich cement lower their individual hydration degree compared to those in OPC, but not the total hydration of cements. Moreover, their proportions influence the microstructure of the hydrated cement: FC produces denser microstructure at an early

age compared to OPC, whereas it is the opposite at a later age. Fe-siliceous hydrogarnet was the main Fe-containing phase in the hydration of the ferrite phase and was quantified by selective dissolution approach. Fe-siliceous hydrogarnet was formed starting from the initial stages of hydration and reached a steady state in approximately 14 days. A high amount of ferrite present in FC enhances the formation of Fe-siliceous hydrogarnet. Fe uptake by C-S-H was estimated from the hydration of ferrite and the amount of formed Fe-siliceous hydrogarnet. A distribution coefficient (R_d) was calculated for the uptake and was related to the equilibrium concentration of Fe ions in the pore solution. Fe(III) ions exist as $Fe(OH)_4^-$ in the high-pH pore solution of the hydrated cement, and C-S-H uptakes $Fe(OH)_4^-$ via surface complexation reactions. The distribution coefficient (R_d) equation was incorporated into the thermodynamic model to predict the hydration products. The experimentally determined Fe-siliceous hydrogarnet and other hydration products agree well with the predicted results for both types of cements. Furthermore, the thermodynamic model predicted that approximately 2 wt.% of Fe was incorporated in C-S-H. Finally, the model efficiently predicted porosity development, and the predicted results were compared with the experimental MIP data.

References

[1] Gagg CR. Cement and concrete as an engineering material: An historic appraisal and case study analysis. Eng Fail Anal 2014; 40:114–40.

[2] Alshalif AF, Irwan JM, Othman N, Al-Gheethi AA, Shamsudin S. A systematic review on bio-sequestration of carbon dioxide in bio-concrete systems: a future direction. Eur J Environ Civ Eng 2020.

[3] Benhelal E, Zahedi G, Hashim H. A novel design for green and economical cement manufacturing. J Clean Prod 2012;22:60–6.

[4] Monteiro P. J. M, Miller S. A, Horvath, A., Towards sustainable concrete, Nature Materials 2017; 16, 698-699.

[5] Morin V, Termkhajornkit P, Huet B, Pham G. Impact of quantity of anhydrite, water to binder

ratio, fineness on kinetics and phase assemblage of belite-ye'elimite-ferrite cement. Cem Concr Res 2017;99:8–17.

[6] Lothenbach B, Scrivener K, Hooton RD. Supplementary cementitious materials. Cem Concr Res 2011;41:1244–56.

[7] Folliet M, Saiz MR, Shah JI. mprovingThermal and Electric Energy Efficiency at Cement Plants: International Best Practice. 2017.

[8] Chabayashi T, Nagata H, Shinmi T, Kato H. Burning test result of the low burning-temperature type clinker by actual kiln and properties of the cement. Cem Sci Cocrete Technol 2015;69:124–30.

[9] Dilnesa BZ, Lothenbach B, Le Saout G, Renaudin G, Mesbah A, Filinchuk Y, et al. Iron in carbonate containing AFm phases. Cem Concr Res 2011;41:311–23.

[10] Elakneswaran Y., et al., "Characteristics of Ferrite-Rich Portland Cement: Comparison With Ordinary Portland Cement," Front. Mater. 2019, vol. 6, no. 97, pp. 1–11, 2019.

[11] Gartner, E., and Myers, D. Influence of tertiary alkanolamines on portland cement hydration. J. Am. Ceram. Soc. 1993;76, 1521–1530.

[12] Schwarz, W. Novel cement matrices by accelerated hydration of the ferrite phase in Portland cement via chemical activation: kinetics and cementitious properties. Advn CemBas Mat. 1995; 2, 189–200.

[13] Dilnesa BZ, Wieland E, Lothenbach B, Dähn R, Scrivener KL. Fe-containing phases in hydrated cements. Cem Concr Res 2014;58:45–55.

[14] Lothenbach B, Zajac M. Application of thermodynamic modelling to hydrated cements. Cem Concr Res 2019;123:105779.

[15] Lothenbach B, Matschei T, Möschner G, Glasser FP. Thermodynamic modelling of the effect of temperature on the hydration and porosity of Portland cement. Cem Concr Res 2008;38:1–18.

[16] Lothenbach B, Kulik DA, Matschei T, Balonis M, Baquerizo L, Dilnesa B, et al. Cemdata18:

A chemical thermodynamic database for hydrated Portland cements and alkali-activated materials. Cem Concr Res 2019;115:472–506.

[17] Vespa M, Wieland E, Dähn R, Lothenbach B. Identification of the Thermodynamically Stable Fe-Containing Phase in Aged Cement Pastes. J Am Ceram Soc 2015;98:2286–94.

[18] Möschner G, Lothenbach B, Winnefeld F, Ulrich A, Figi R, Kretzschmar R. Solid solution between Al-ettringite and Fe-ettringite (Ca6[Al1 - xFex(OH)6]2(SO4)3·26H2O). Cem Concr Res 2009;39:482–9.

[19] Mancini A, Wieland E, Geng G, Dähn R, Skibsted J, Wehrli B, et al. Fe(III) uptake by calcium silicate hydrates. Appl Geochemistry 2020;113:104460.

[20] Labhasetwar NK, Shrivastava OP, Medikov YY. Mössbauer study on iron-exchanged calcium silicate hydrate: Ca5-xFexSi6O18H2 · nH2O. J Solid State Chem 1991;93:82–7.

[21] Faucon P, Le Bescop P, Adenot F, Bonville P, Jacquinot JF, Pineau F, et al. Leaching of cement: Study of the surface layer. Cem Concr Res 1996;26:1707–15.

[22] Elakneswaran Y, Owaki E, Miyahara S, Ogino M, Maruya T, Nawa T. Hydration study of slag-blended cement based on thermodynamic considerations. Constr Build Mater 2016;124:615–25.

[23] Charlton, S.R., Parkhurst, D.L. Modules based on the geochemical model PHREEQC for use in scripting and programming languages, Comput. Geosci 2011. 37, 1653–1663.

~~[24] Lothenbach, B. et al. Cemdata18: A chemical thermodynamic database for hydrated Portland cements and alkali-activated materials. Cement and Concrete Research 2019. 115, 472-506.~~

~~[25] Lothenbach, B. et al. Thermodynamic Modelling of the Effect of Temperature on the Hydration and Porosity of Portland Cement. Cement and Concrete Research 2008. 38 (1), 1–18.~~

[26] Parkhust, D. L., Appelo, C. A. J. A computer program for speciation, batch-reaction, one-dimensional transport and inverse geochemical calculations. USGS report., 1999

[27] Hong, S. Y. and Glasser, F. P., Alkali binding in cement pastes Part I. The C-S-H phase, Cem. Concr. Res. 1999, vol. 29, pp. 1893–1903.

[28] Chen. W. and Brouwers, H. J. H., Alkali binding in hydrated Portland cement paste, Cem. Concr. Res. 2010, vol. 40, pp. 716–722.

[29] Émilie Michèle L'HÔPITAL, Aluminium and alkali uptake in calcium silicate hydrates (C-S-H), PhD thesis, ÉCOLE POLYTECHNIQUE FÉDÉRALE DE LAUSANNE, 2014.

[30] Li, J et al., The chemistry and structure of calcium (alumino) silicate hydrate: A studyby XANES, ptychographic imaging, and wide- and small-angle scattering, Cement and Concrete Research 2019. 115. 367-378.

[31] Hass, J and Nonat, A. From C–S–HtoC–A–S–H: Experimental study and thermodynamic modelling, Cem. Concr. Res. 2015. 68. 124-138

[32] Elakneswaran, Y et al. Electrokinetic potential of hydrated cement in relation to adsorption of chlorides, Cem. Concr. Res. 2009. 39. 340-344.

[33] Matschei, T. Lothenbach, B. and Glasser, F. P. The AFm phase in Portland cement," Cem. Concr. Res. 2007, vol. 37, no. 2, pp. 118–130.

[34] Siventhirarajah K., Yoda Y., Elakneswaran Y., A two-phase model for the prediction of mechanical properties of cement paste, Cement and Concrete Composites. 2021, 115, 103853.